Proceedings of the Second International Workshop on EGS, 8.-12. August 2000, Tsukuba, Japan
KEK Proceedings 200-20, pp.23-30

Application of EGS4 Code to Whole-body Counting

S. Kinase, M. Yoshizawa, J. Kuwabara and H. Noguchi

Japan Atomic Energy Research Institute
Tokai-mura, Naka-gun, Ibaraki-ken 319-1195, Japan

Abstract

The authors have applied the EGS4 code to the evaluation of the responses of a whole-body counter using mathematical models and correction factors for individuals in order to improve accuracy on the assessment of body burdens. It was found that the calibration of the whole-body counter by the EGS4 code could replace the actual calibration and the calculated correction factors shall be practical and useful for the whole-body counting.

1 Introduction

A whole-body counter is used for direct measurement of body radioactivity made in programmes of internal dosimetry for occupational radiation monitoring. The apparatus is useful for identification, quantification and location of radionuclides in the body, but there is need for previous calibration of the detection equipment with proper phantoms containing standard sources of the required radionuclides. It is very difficult that a single institution prepares many kinds of phantoms containing radionuclides for the calibration. Hence, it is necessary to find a calibration method for the whole-body counter without using any phantoms.

Previous works [1,2] have developed Monte Carlo simulation codes for the calibration of whole-body counter. They have demonstrated the possibility of a calibration method for whole-body counters using Monte Carlo technique. However, the simulations did not consider the energy resolution of the detectors. The calibrations by the simulations could not replace those by actual measurements.

We have applied the EGS4 code to the calibration of a whole-body counter installed in the Japan Atomic Energy Research Institute (JAERI) in order to improve accuracy on the assessment of body burdens [3,4,5]. The present paper describes the feasibility of the calibration method using the EGS4 code, responses of the whole-body counter regarding distributions of radioactivity and correction factors for individuals by comparing of the calculated and measured response functions.

2 Materials and Methods

2.1 Whole-body counter and phantom

JAERI has a precision whole-body counter that is shown in Photo 1. It has three parts: shielding, detectors and analyzers. The shielding consists of a steel room whose walls, ceiling and floor are 21 cm-thick. The inner sides of the room are lined with 3 mm-thick lead. The internal dimensions are 200 (height) $\times$ 80 (width) $\times$ 200 (length) cm^3. The detectors are five cylindrical 20.32-cm-diameter $\times$ 10.16-cm-length thallium-activated sodium iodide [NaI(Tl)] crystals in a fixed geometry. The electrical signals from the detectors are transmitted to a multichannel analyzer which displays pulse height spectra.

The sensitivity along longitudinal axis of the body to a ^{137}Cs point source is uniform with an arrangement of the subject-detector configuration. The distance from each of the NaI(Tl) crystals facing the subject is between 6.7 and 10.5 cm.

The whole-body counter is calibrated by placing known amounts of a radionuclide in a water-filled block-shape phantom whose size is fitted to the average size of workers in JAERI. The phantom consists of thirteen vessels of rectangular cross-section. Each vessel is filled with a radionuclide in solution. The wall of the vessel made of vinyl chloride is 5 mm in thickness. The phantom is usually placed on a bed under the condition that the neck part was directly over the extreme of the detectors array.

JAERI makes it a rule to measure subjects in a supine posture for 1,000 seconds in individual monitoring programmes for internal exposure of radiation workers.

2.2 Monte Calro simulations

Monte Carlo simulations were carried out using the EGS4 code system [6] in conjunction with a user code for general purpose (UCGEN) [7]. The photon cross sections for materials were taken from PHOTX [8].The number of history of the simulations was determined to be a million in order to reduce statistical uncertainties. The response functions calculated by the EGS4 code were folded with a Gaussian distribution since the energy resolution of the detector is not considered by the EGS4 code [9].

2.2.1 A calibration method using the EGS4 code

Figure 1 shows the calculation geometry of the whole-body counter and the water-filled block-shape phantom (hereafter adult water phantom) in JAERI, which is used for the Monte Carlo simulation.

The counting efficiencies ε (counts$\cdot$s$^{-1}\cdot$Bq^{-1}) of the whole-body counter were obtained by

$$\varepsilon = \sum_{k=a}^{b} n_k / A, \tag{1}$$

where n_k is the number of photons of the energy k in the detectors, a the lower energy of the peak, b the upper energy of the peak and A the number of photons generated in the phantom. The lower and upper energies of the peak were determined to be double the FWHM of the peak.

In addition to the adult water phantom, to study geometry and source effects, two kinds of phantoms were modeled on the basis of the report by Hayes [10]: child and adolescent water phantoms. The size of the above three phantoms are shown in Table 1.

Furthermore, for quantitatively investigating the scattering effect of photons, the full-energy peak efficiencies (hereafter peak efficiencies) ε' (counts$\cdot$s$^{-1}\cdot$Bq^{-1}) were also calculated by

$$\varepsilon' = n / A, \tag{2}$$

where n is the number of photons as the full-energy peak counts of the response function that was not folded.

To validate the simulations, calculated response functions for the adult water phantom (^{137}Cs, ^{40}K) were compared with measured ones.

2.2.2 Responses of the whole-body counter regarding distributions of radioactivity

Responses of the whole-body counter regarding various ^{137}Cs distributions within an anthropomorphic phantom were evaluated by simulations. The phantom was a MIRD-5 type phantom [11,12]. The distribution of ^{137}Cs within the MIRD-5 type phantom was determined to be variable on the basis of the ratio of ^{137}Cs between in the stomach region and in the whole-body since Cs is distributed uniformly throughout the body [13] and Iinuma et al. [14] showed that a large amount of ^{137}Cs remained in the region of the stomach and small intestine for 2 or 3 days after oral administration. When ^{137}Cs was present within the whole-body except for the stomach region, the ratio of ^{137}Cs concentration was set to be lung, 0.07: skeleton/soft tissue, 1.00. It was determined on the basis of ICRP Reference Man [13] whose ratio of Cs concentration was lung, 0.07: skeleton, 0.90: soft tissue, 1.00.

2.2.3 Correction factors for individuals

To study the correction factor of the counting efficiency on ^{40}K, of which activity in the body is dependent on the individuals, counting efficiencies of the whole-body counter to the above three water phantoms were evaluated by simulations. The surface area of the subjects was chosen as the correction factor since Komiya et al. [15] presented that total body water and percent fat could be predicted from the surface area. A polynomial regression equation as a function of the surface area of the phantom was derived to obtain the applicable counting efficiencies for individuals of different sizes. The surface area is expressed by the equation [13]:

$$X = 0.0072 \cdot W^{0.425} \cdot H^{0.725} \tag{3}$$

where X is the surface area (m^2), W the weight (kg) and H the height (cm).

To demonstrate the correction factors, the ^{40}K contents in the total body of Japanese male adults 50 were measured with the whole-body counter, and the ^{40}K contents corrected by using the correction equation were compared with the not corrected ^{40}K contents.

3 Results and Discussion

3.1 A calibration method using the EGS4 code

Figure 2 shows the calculated and the measured response functions for the ^{137}Cs adult water phantom. The fractional standard deviation at a peak of 662 keV of the calculated response function that was not folded was 0.69 %. It can be seen that the calculation agrees very well with the measurement.

Figure 3 shows the calculated counting efficiencies ε curves for the child, adolescent and adult water phantoms and the measured counting efficiencies for the adult water phantom. The calculated counting efficiencies for the adult water phantom are in fairly good agreement with the measured ones. The calculated counting efficiency curves are nearly straight in the photon energy range of 300-1,461 keV. The calculated counting efficiency ε decreases with an increase in photon energy in all energy range. The peak efficiencies ε' are also shown in the figure. The peak efficiency ε' increases up to about 500 keV photon energy and then decreases. The difference between ε and ε' is attributed to the determination of the peak counts; counts due to scattering of photons included in the peak counts for ε, but not for ε' calculated with the full-energy peak counts. The influence of the scattering effect of photons on the counting efficiency regarding the child, adolescent and adult water phantoms accounts for 10 $\pm$ 1 % of the counting efficiency for 662 keV photons.

3.2 Responses of the whole-body counter regarding distributions of radioactivity

Figure 4 shows the variation of counting efficiency of the whole-body counter with the ratio of ^{137}Cs between in the stomach region and in the whole-body (Stomach/Whole body) for the MIRD-5 type phantom. Each of counting efficiencies for various distributions is normalized against that for the whole-body distribution. The response of the whole-body counter decreases as shown in Fig. 4 as ^{137}Cs in the stomach region increases against that in the whole-body. The counting efficiency for the only stomach region is about one third of that for the whole-body.

3.3 Correction factors for individuals

Figure 5 shows the relationship between the surface area of water phantoms and their counting efficiencies. Each counting efficiency is normalized to that of the adult water phantom. It was found from the calculation that the counting efficiencies decrease with increasing surface area of the phantom. The relationship is expressed as a polynomial regression curve by the following equation:

$$Y = -1.654 \cdot 10^{-1} \cdot X^2 + 5.190 \cdot 10^{-2} \cdot X + 1.371 \tag{4}$$

where Y is the counting efficiency ratio and X the surface area of the phantom (m^2).

The relationship between the ^{40}K contents in the total body and the lean body mass (LBM) of the 50 subjects is shown in Fig. 6 along with the regression lines and correlation coefficients (r). In the figure, the heavy solid line represents the relationship between the LBM and the ^{40}K contents in the total body on the following assumptions: the adipose tissue has much less K contents than the LBM and the LBM contains, on the average, 2.663 g $K \cdot kg^{-1}$ [16]. The corrected ^{40}K contents for the LBM give higher correlation coefficient than the non-corrected contents. The r values of the corrected and the non-corrected ^{40}K contents for the LBM in regression are 0.90 and 0.69, respectively. It can be seen that the slope of the regression equation on the corrected ^{40}K contents is similar to that of the heavy solid line.

4 Conclusions

The EGS4 code was applied to the calibration of the JAERI whole-body counter. The following conclusions were derived.

1. The calibration method by the calculation was validated by comparing of the calculated and measured response functions. The calculated counting efficiencies are useful for routine and unusual measurements. The counting efficiency curves for the child, adolescent and adult water phantoms are nearly straight in logarithmic scale in the photon energy range 300-1,461 keV when the peak counts integrated between double the FWHM of the peak. The scattering effect of photons on the counting efficiency regarding the water phantoms accounts for 10 $\pm$ 1 % of the counting efficiency for 662 keV photons.

2. The counting efficiencies of the whole-body counter strongly depend on the ^{137}Cs distribution within the body. The ^{137}Cs body burdens would be underestimated by a factor of 3 in the worst case.

3. Using the calculated counting efficiencies, the correction factors on ^{40}K whole-body counting were determined. The correction factors for the ^{40}K whole-body counting shall be practical and useful for the JAERI whole-body counter.

References

[1] J. G. Hunt, et al., "Calibration of in vivo measurement systems and evaluation of lung measurement uncertainties using a voxel phantom", *Radiat. Prot. Dosim.* **76**(1998)179-184.

[2] T. Ishikawa et al., "A calibration method for whole-body counters, using Monte Carlo simulation", *Radiat. Prot. Dosim.* **64**(1996)283-288.

[3] S. Kinase, "Evaluation of response of whole-body counter using the EGS4 code", *J. Nucl. Sci. Technol.* **35**(1998)958-962.

[4] S. Kinase, "Correction factor for potassium-40 whole-body counting", *J. Nucl. Sci. Technol.* **36**(1999)952-956.

[5] S. Kinase, "Response function simulation for a whole-body counter", Proceedings of the eighth EGS4 users' meeting in Japan, Tsukuba, August 1999, KEK Proceedings 99-15, 76-81 (1999).

[6] W. R. Nelson, et al., "The EGS4 code system", *SLAC-265* (1985).

[7] I. Nojiri et al., "Development of EGS4 user's code for general purpose", *Dounengihou* **102** (1997)59-66, (in Japanese).

[8] PHOTX : RSIC Data Package, DLC-136(1989).

[9] K. Saito and S. Moriuchi, "Data catalog of gamma ray response functions for NaI(Tl) scintillation detectors by the Monte Carlo calculation", *JAERI-1306*(1987), (in Japanese).

[10] R. L. Hayes, "Standard-man phantoms", *ORINS-35*(1960).

[11] W. S. Snyder et al., "Estimates of specific absorbed fractions for photon sources uniformly distributed in various organs of heterogeneous phantom", *NM/MIRD Pamphlet No.5* (revised), *J. Nucl. Med.* **19**, Supplement 5-67 (1987).

[12] O. Sato, et al., "Calculation of equivalent dose and effective dose conversion coefficients for photons from 1MeV to 10 GeV", *Radiat. Prot. Dosim.* **62**(1995)119-130.

[13] "ICRP. Reference Man : Anatomical, Physiological and Metabolic Characteristic", *Publication 23* (Oxford : Pergamon Press) (1974).

[14] T. A. Iinuma et al., "Application of metal ferrocyanide-anion exchange resin to the enhancement of elimination of ^{137}Cs from human body", *Health Phys.* **20**(1971)11-21.

[15] S. Komiya et al., "Equation for estimating percent fat of Japanese men", *J. Physical Fitness Japan* **34**(1985)259-268, (in Japanese).

[16] G. B. Forbes et al., "Effects of body size on potassium-40 measurement in the whole body counter (tilt-chair technique)", *Health Phys.* **15**(1968)435-442.

Table 1 The water phantoms for the Monte Carlo simulation

	Adult			Adolescent			Child		
Parts	Height (cm)	Width (cm)	Length (cm)	Height (cm)	Width (cm)	Length (cm)	Height (cm)	Width (cm)	Length (cm)
Head	16.7	13.3	18.0	15.8	12.4	17.9	14.0	11.5	16.8
Neck	8.7	7.8	8.5	7.2	6.7	7.6	5.2	4.9	5.7
Chest	19.4	29.1	20.3	17.1	23.9	17.8	12.0	16.0	12.0
Abdomen	16.1	25.0	20.3	14.2	21.3	17.8	12.7	16.0	12.0
Arm	7.4	6.6	51.0	5.8	5.1	45.3	4.4	4.0	28.0
Pelvis	18.8	28.2	23.6	15.0	23.8	20.6	13.9	16.0	14.0
Thigh	12.7	11.4	33.0	10.5	9.4	27.5	6.8	6.1	14.0
Lower leg	8.6	7.7	37.7	6.8	6.1	34.4	5.1	4.6	19.0
Foot	16.8	8.4	6.6	12.9	6.9	5.8	9.5	5.0	4.5
Height	168.0 cm			149.4 cm			98.0 cm		
Weight	60.2 kg			37.4 kg			14.9 kg		

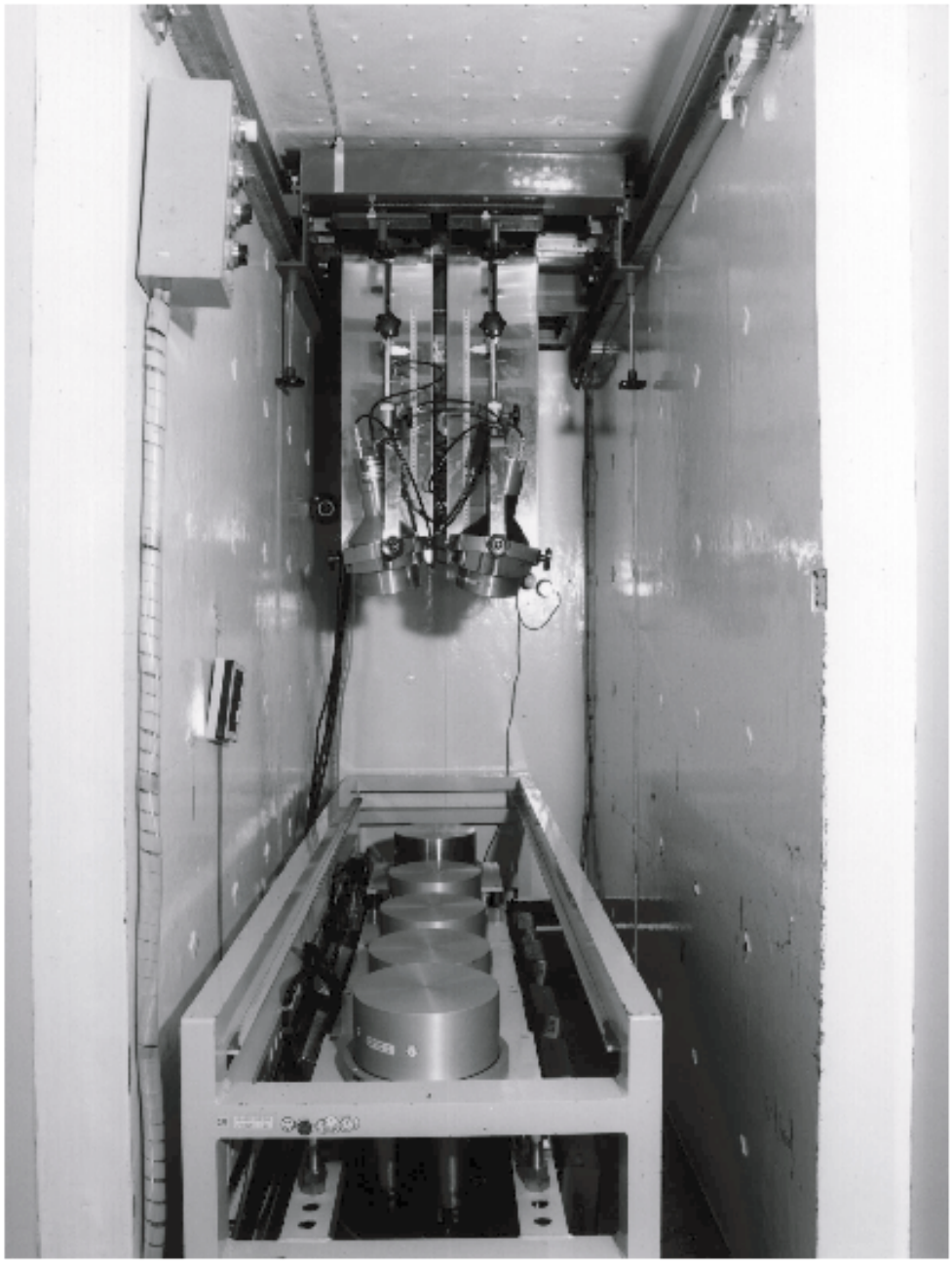

Photo.1 A photograph of a whole-body counter in JAERI.

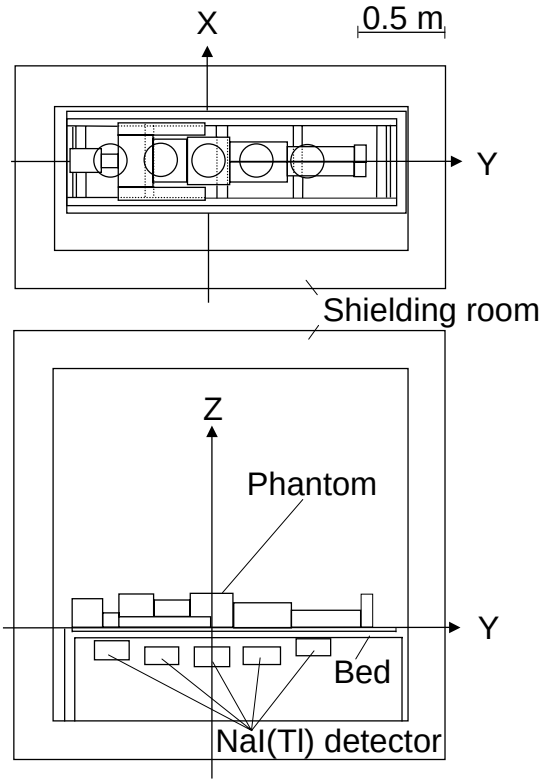

Figure 1: Geometry of the JAERI whole-bidy ciunter and adult water phantom.

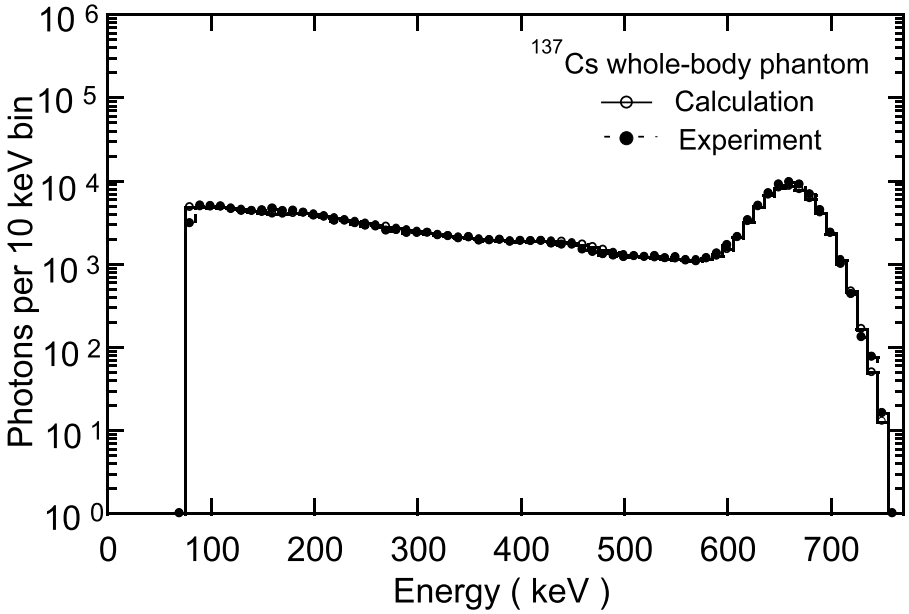

Figure 2: Comparison of the calculated and measured response functions for the adult water phantom.

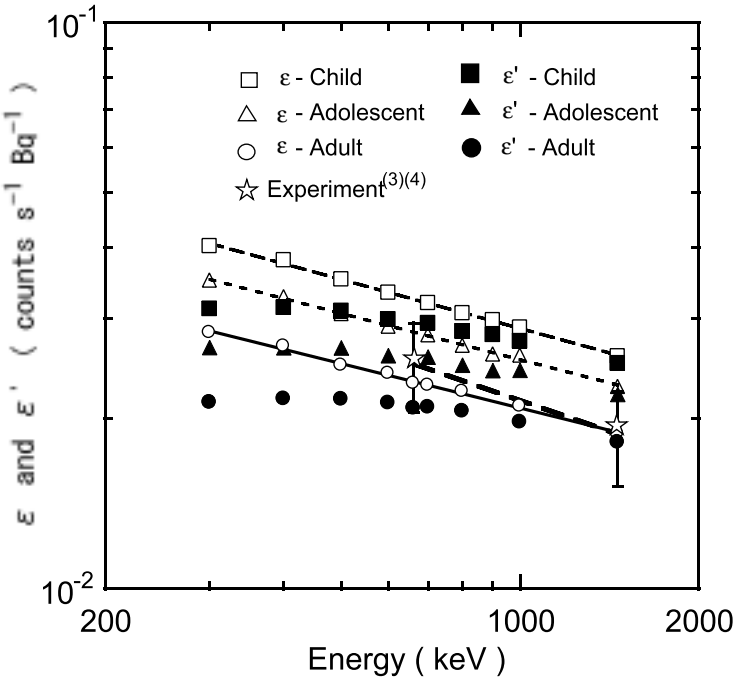

Figure 3: Counting efficiencies ε and peak efficiencies ε' of the JAERI whole body counter for the child, adolescent and adult

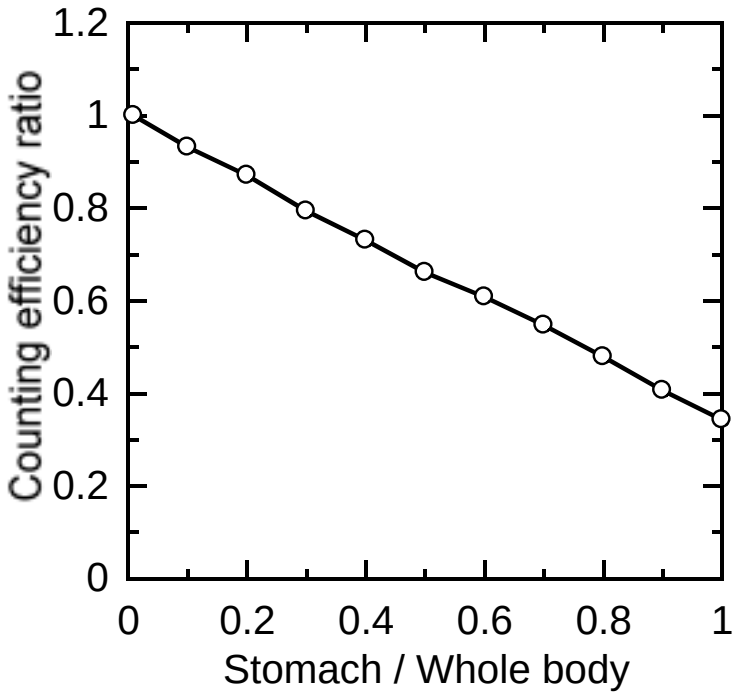

Figure 4: Response of the JAERI whole-body counter regarding various ^{137}Cs distributions.

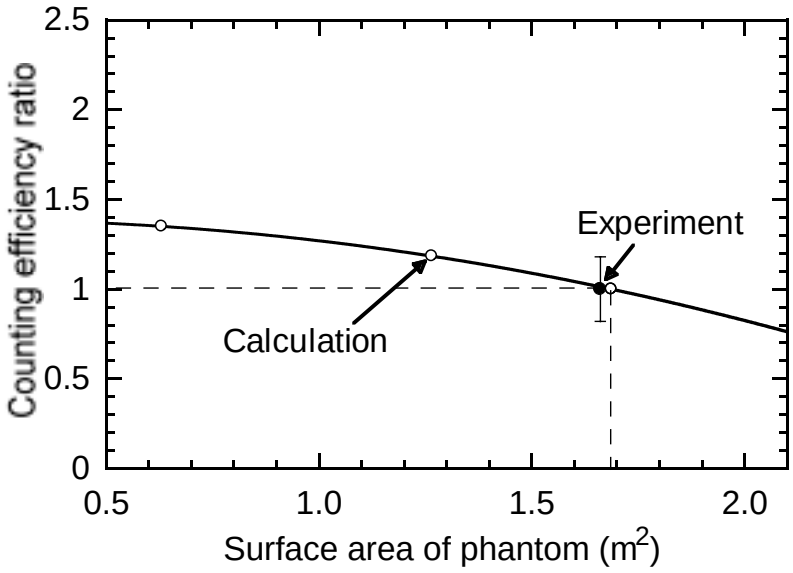

Figure 5: Counting efficiency of the JAERI whole-body counter regarding the surface area of the watewr phantom.

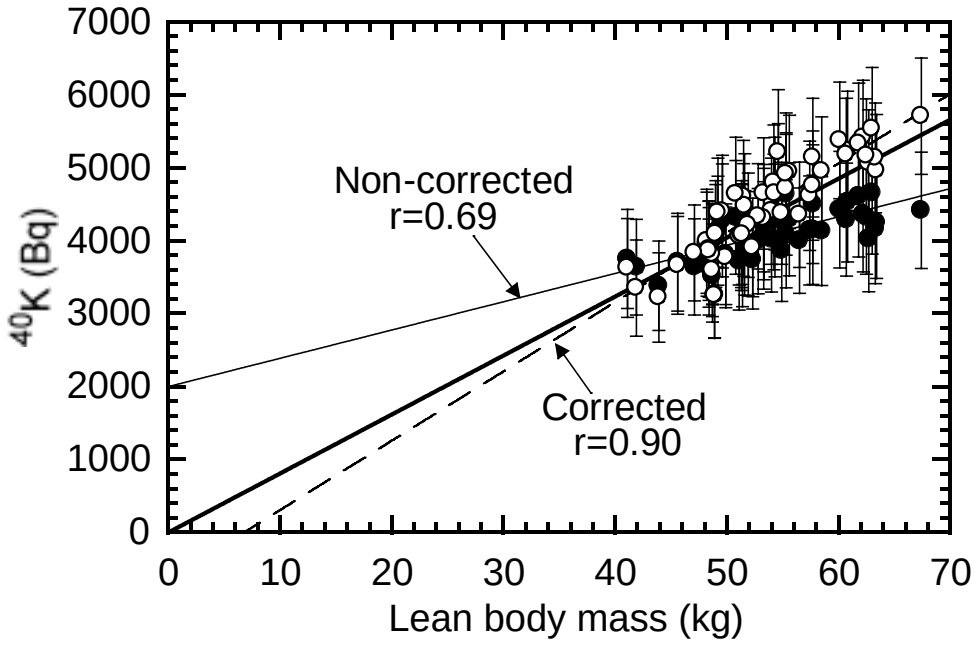

Figure 6: Relationship between the ^{40}K contents in the total body and the lean body mass.